



PHYSICAL PROCESSES AND MATERIALS IN HIGH-ENERGY FLUXES PROCESSING

Peter Petrov^{*}, Stefan Valkov, Maria Ormanova, Darina Kaisheva, Todor Hikov

Institute of Electronics, BAS, Tsarigradsko Chaussee 72, 1784 Sofia, Bulgaria

ARTICLE INFO

Article history:

Received 1 October 2018

Accepted 20 November 2018

Keywords:

electron and photon beams, welding, treatment and alloying.

ABSTRACT

The present stage of scientific and technological development is characterized by wide-ranging and diverse applications of the energy of high-energy fluxes (HEFs), such as electron and photon beams. The fundamental advantage of HEFs over the conventional heat sources is the possibility to achieve high energy density on the surface of the component treated, which explains the wide use of HEFs for welding, heat treatment, surface modification, fabrication of wear- and corrosion-resistant coatings, etc.

The use of HEFs for modification of metal and alloys widens the capabilities of the techniques for improving their physical and mechanical properties. In recent years, as the studies on the development of novel materials have intensified, hybrid techniques of HEFs treatment began to be widely applied, whereby additional alloying is performed in the treated zone thus achieving a substantial effect on the physical and mechanical properties of the materials processed.

This work presents results HEFs modification and welding of metals and alloys obtained in recent years at the Laboratory of Physical Technologies at the Institute of Electronics of the Bulgarian Academy of Sciences

© 2018 Journal of the Technical University of Gabrovo. All rights reserved.

INTRODUCTION

The high-energy fluxes (HEF), e.g. electron, photon and ion beam have been used in many branches of the industry. The small size of the treated zone and the high density of the surface energy of the details which have been treated make the difference between the high-energy fluxes (HEF) and conventional method. For that reason HEF are widely used for surface modification, formation of wear resistant and corrosion resistant hard layers, welding etc.

The Institute of Electronics in its branch laboratory "Physical technologies", has well-recognized achievements both in Bulgaria and abroad in the field of direct current (DC) reactive magnetron sputtering and electron beam technology. Recent investigations, are focusing mainly on:

- Development and studies of novel materials with applications in nanotechnologies and nano-electronics.
- Studies of physical processes and materials; development of technologies for selective alloying, surface modification and welding by electron and photon beams.
- Neutronography studies of condensed matter.
- Preparation and studies of single- and multi-layer nitride (TiN, CrN, AlN, ZrN, VN, WN, MoN, NbN, HfN, TiN/WN, TiN/CrN, TiN/ZrN) and oxide (TiO₂, Al₂O₃, CuO, PbO, NiO₂, CrO₂, Ta₂O₅, TiN/TiO₂) wear-resistant coatings with applications in bio-medicine, and for optical lenses, selective filters and screen protection.
- Development of technologies for deposition of coatings on textiles, hard polymer and polymer-foil packaging materials, ultra-filtration polymer membranes.

ELECTRON BEAM ALLOYING

The alloying processes are based on the melting of the surface of the alloyed material and applying alloying elements into the melt pool which are dissolved into the matrix of the based material and forming surface alloys. The alloying material can be applied previously in the form of coatings by means of other techniques (e.g. magnetron sputtering, plasma spraying, etc.) or can be incorporated into the melt pool directly in the form of a powder stream or wire.

The high energy fluxes alloying techniques are widely used for fabrication of materials for the needs of the automotive and aerospace industries, for manufacturing of railway cars, space crafts, light ships etc. Such materials are aluminum alloys due to their attractive mechanical properties and light weight. Alloying of pure aluminum with different transition metals by means of high energy fluxes is among the most promising methods for fabrication of surface alloys and for improvement of the surface properties of the materials. For that reason many researchers are working on the formation and characterization of surface alloys by high energy fluxes.

The alloying of titanium and titanium alloys is a subject of investigations for many scientists due to the application of these materials in the field of the contemporary aviation and automotive industries, for different biomedical applications and many more.

The authors of [1] have studied an electron beam surface alloying of pure Ti with Al films and their results

^{*} Corresponding author. E-mail: pitiv@ie.bas.bg

show that the alloyed zone consists of biphasic structure of Ti₃Al and TiAl which is transformed in single phase structure of TiAl in depth. This transformation is accompanied by a decrease in the hardness from the surface to the depth. Also, the authors of [2] have studied the conditions of alloying of pure Ti with Al and Nb and with Al and V. The results showed that the formation of an intermetallic surface alloy by means of electron beam alloying strongly depends on the input energy of the e-beam. The same authors [2] have claimed that the melting point of the materials plays a major role in the optimization of the technological parameters of a selective electron beam technology. The authors of [3] have demonstrated an electron beam additive technique for formation of Ti-Al-Nb surface alloys. It was realized cycling mixing of predeposited bilayer of Al/Nb

coating with pure Ti substrate by selective electron beam melting SEBM where the maximum number of the cycles is 3. The first one was a SEBM of the deposited bilayer with the Ti substrate. The second cycle was a SEBM process of the same bilayer coating of Al/Nb deposited on the already formed by the first one surface alloy and the same procedure was repeated for the third one. The results obtained in [3] showed that Ti₂AlNb based phases has been formed and the microhardness of 180 HV for the pure Ti substrate increases to 570 HV after the third

cycle. A scheme of cycling mixing of the predeposited Al/Nb coating with pure Ti is presented in Fig. 1.

As already mentioned, the modification of aluminum for improving of its operational characteristics is also a subject of investigations in the field of the modern materials science.

In [4] it has been demonstrated a modification of the mechanical properties of pure Al by incorporation of TiCN nanopowder by means of electron beam alloying. Their results show that the alloyed zone has a thickness in the range of 14-33 μm and microhardness from 562 HV to 798 HV or the alloyed zone is 16-22 times harder than the base Al substrate.

Some authors have studied laser beam surface alloying of Al with Cr using two-step process (alloying and remelting) [5]. The results show that an increase of the remelting speed, points to an increase in the volume fraction of the intermetallic compound and the hardness, respectively. In studies [6-9] it has been investigated an alloying of pure Al with Nb by means of laser alloying technique. The results obtained by the authors show that the distribution of the alloying element is not homogeneous and undissolved Nb particles surrounded by dendrites of Al₃Nb exist. Fig. 2 presents undissolved Nb particle surrounded by Al₃Nb dendrites.

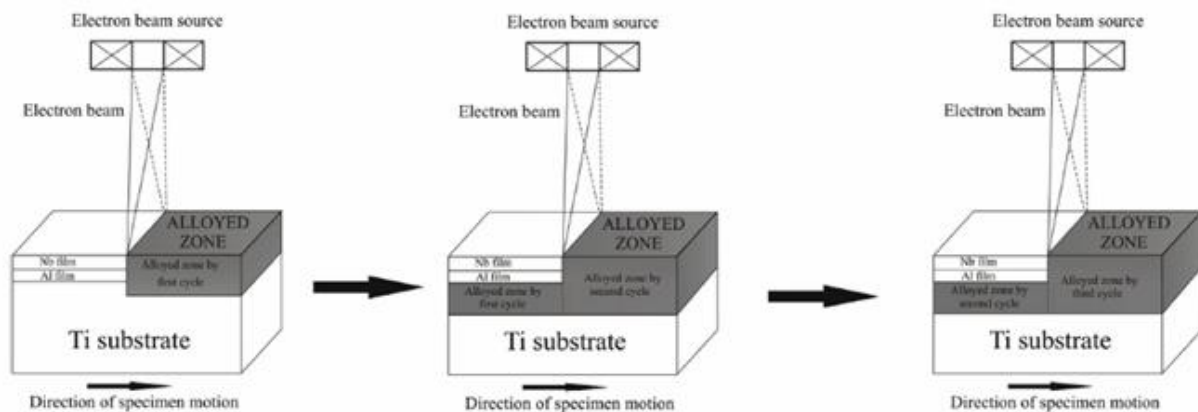


Fig. 1. A scheme of cycling electron-beam liquid mixing of Al/Nb coating with Ti substrate [3]

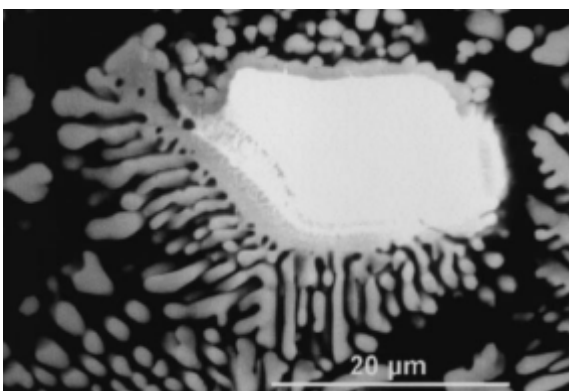


Fig. 2. Undissolved Nb particle surrounded by Al₃Nb dendrites [9]

However, the characteristics of the alloyed layers were greatly improved after a laser remelting. Most of the structural defects were eliminated and undissolved Nb particles have not been observed. The manufactured laser-

beam surface alloys have been successfully formed with an Al₃Nb dendritic microstructure. The same authors [9] claimed that the microhardness increases with an increase of the scanning speed during the laser alloying technology. The reported microhardness changes from 480 HV to 650 HV with varying of the scanning speed from 5mm/sec to 40 mm/sec.

The work [10] presents an alloying of pure aluminum with as-deposited Ti/Nb coatings by means of a scanning electron beam and their results show that undissolved particles have not been observed after the alloying process, contrary to the case of laser beam alloying. The alloyed zone consists of (Ti,Nb)Al₃ intermetallic fractions randomly distributed in the biphasic structure of fine (Ti,Nb)Al₃ particles dispersed in the Al matrix. The microstructure of the obtained surface alloy is presented in Fig. 3.

The increase of the scanning speed tends to more homogeneity distribution of the intermetallic phase in the soft Al matrix and much finer microstructure. Also, the measured microhardness reaches values of 775 HV and it is

not depend on the scanning speed during the electron-beam alloying process. Therefore, a significant difference between the properties and structure of the fabricated surface alloys by electron and laser beam exist. The authors of [11] have made a comparative study of electron and laser beam surface alloying of pure Al with Nb. The results reported in [11] have shown that the observed differences in the microstructure of the surface alloys formed by both techniques are explained by the different way of controlling the lifetime of the melt pool. The electron-beam alloying technique can be realized in different geometries of scanning (circular, linear, etc.) since the electrons can be deflected and guided due to their nature of charged particles. When using circular scanning mode, the trajectory of the e-beam overlaps which points to longer lifetime of the melt pool. Using laser beam alloying technique, such technological conditions cannot be realized and the lifetime of the melt pool is significantly shorter [11]. The authors of [12, 13] have performed detailed investigations of the microstructure and the crystallographic structure of surface alloys fabricate by electron and laser beam alloying and explain the difference in the hardening mechanism of both kind of alloys. Also, in [12] it has been studied the crystallographic structure of laser beam manufactured surface alloys and their results show that the increase of the scanning speed during the alloying process reflects to formation of a preferred crystallographic orientation while such effect of electron-beam fabricated surface alloys has not been observed [13]. According to the authors of [14, 15] the formation of a preferred crystallographic orientation can significantly affect the mechanical properties which, as mentioned in [13] can be a possible reason for the observed differences in the hardening mechanism of electron and laser processed surface alloys.

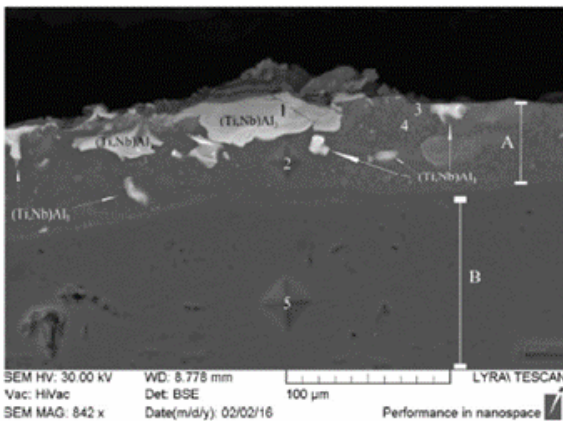


Fig. 3. Microstructure of Al-Ti-Nb surface alloy formed by electron-beam alloying
A- alloyed layer; B – aluminum substrate [10]

ELECTRON BEAM HEAT TREATMENT

The electron beam heat treatment (EBHT) is widely used for obtaining of modified layers. During this process the flux of accelerated electrons interacts with the surface of the treated materials which forms thermal distribution from the surface to the bulk of the sample as a result of the transformation of the kinetic energy into heat [16-19].

In work [20] we present a combined method for surface modification on tool steel (0,31%C; 0,30%Si; 0,35%Mn; 2,9%Cr; 2,8%Mo; 0,5%V), consisting of electron beam

treatment, plasma nitriding and subsequent electron beam treatment (fig.4).

The results obtained in this study demonstrate a possibility of producing gradient coatings with high hardness by combination of electron beam treatment (EBT) and plasma nitriding (PN). The application of surface treatment by scanning electron beam leads to obtaining finer structure and improvement of the adhesion between the base material and the following coatings.

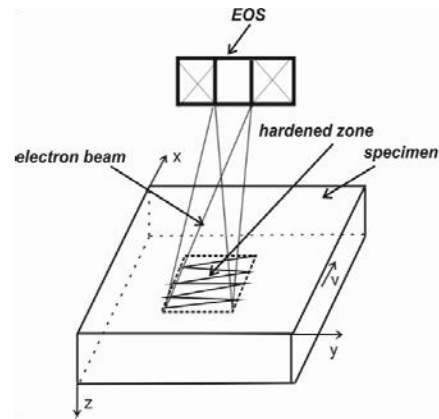


Fig.4. Schematic diagram of scanning electron beam treatment

For that reason, a treatment with scanning electron beam has been chosen before the developing of the nitride coating. The XRD results demonstrate the presence of nitrogen phases – Fe₃N and FeN_{0.076} at samples 1 (EBT+PN) and 2 (EBT+PN+EBT), respectively. After application of the second electron-beam treatment the nitrogen atoms are redistributing and Fe₃N with hexagonal closed-pack (hcp) crystal lattice has been transformed to FeN_{0.076} with face-centered cubic (fcc) structure. This type of treatments makes the structure finer but the grain size of FeN_{0.076} is bigger than that of Fe₃N. After the conducted mechanical investigations, the hardness of EBT+PN is 760 kg/mm² or is about four times greater than the base material. The redistribution of the nitrogen and the bigger grain size of FeN_{0.076} of sample 2 (EBT+PN+EBT) leads to decreasing of the hardness in the zone where the second electron beam treatment (EBT) has been done (range of 5-24 mm) compared to sample 1 (EBT+PN). The application of the plasma nitriding (PN) process after the electron beam treatment (EBT) increases the hardness of the surface layer. The coating obtained after second electron beam treatment (EBT) has a finer grain structure and can serve as a base for deposition of other films with improved properties by different methods (fig.5).

In order to determine the temperature field, and thus - the heating and cooling rates during the electron beam treatment process, experimental and numerical methods are used.

In study [21] we are developed a thermal model, in which the electron beam energy distribution is obtained by taking into account the frequency and amplitude of beam scanning over the different trajectories. The model is based on solving the heat transfer equation by means of the Green functions. The thermal field and the size of the structural changes zone have been calculated for instrumental steel samples.

Fig. 6 shows the distribution of the thermal field in the sample depth from $z = 0$ to $z = 1$ mm, and Fig. 7 – the temperature distribution on the surface, $z = 0$.

It can be seen that the thermal field is highly inhomogeneous and has non-stationary nature. The maximal temperature obtained on the surface of the sample (Fig. 6) is $T = 784,625^{\circ}\text{C}$. The calculated value of the treated zone depth (in the temperature interval $500\text{-}800^{\circ}\text{C}$) is $h_{\text{calc}} \approx 100\mu\text{m}$ (Fig. 7). The layers in the sample depth reach temperature maximum later than the layers close to the surface, the latter having higher heating and cooling rates.

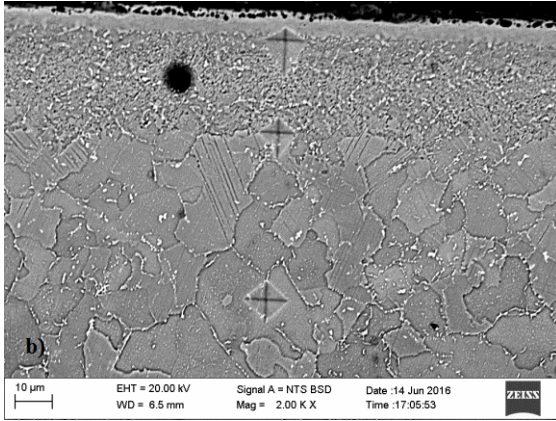


Fig.5. SEM metallographic cross section of EBT+PN+EBT

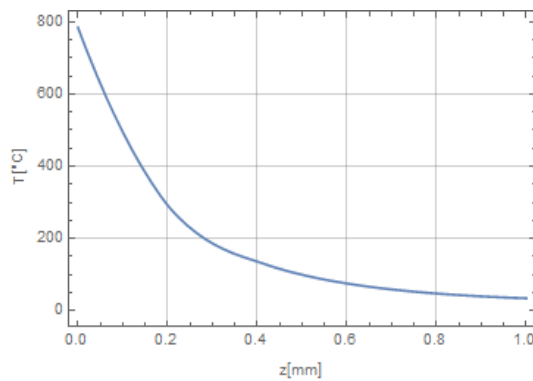


Fig. 6. Temperature distribution in depth, from $z = 0$ to $z = 1$ mm

The comparison of the experimentally obtained with the theoretically calculated zones of thermal treatment and the corresponding structural changes show good agreement.

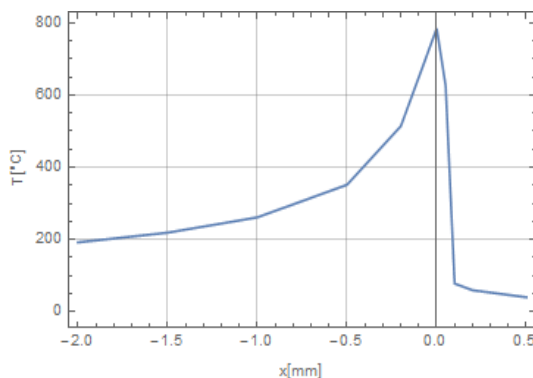


Fig. 7. Temperature distribution at the surface, $z = 0$

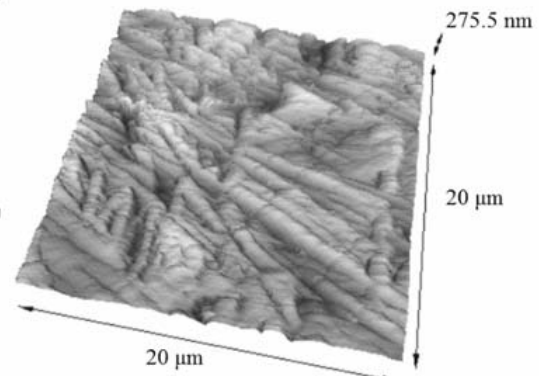
One technique for treating the surface of materials is the use of high-intensity electron beam [22]. The rate of the heating and cooling processes can achieve quite high values (about ~ 106 K/s), which leads to some structural transformations, increase in the hardness and change in

surface topography. The surface modification by this method is based on the effect of creating these protrusions by electron beam scanning. This allows us to scan the surface accurately with high repetition rate and generate whatever pattern is necessary.

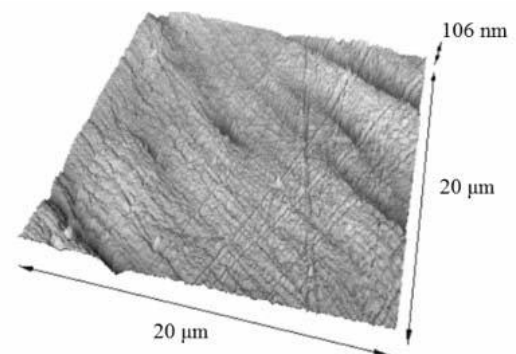
The substrate material used in the present study was Ti5Al4V. The material was electron beam treated (EBT) using the technological parameters described precisely in [23].

After the EBT, the deposition of the multilayered coating took place. It was realized by reactive magnetron sputtering (RMS). The deposition of the TiN layer took place in Ar-N₂ atmosphere, and the working pressure was 1.2×10^{-1} Pa. The TiO₂ film was realized in the pure O₂ environment, the working pressure was 7×10^{-2} Pa. Negative bias voltage to the substrate has not been applied.

First the hardness of the substrates with and without EBT were measured. In all measured cases the values increase after treatment which is due to the transformation $\alpha + \beta$ to α' martensitic microstructure occurring due to the fast cooling rate after the melting process [22]. SEM micrographs (not shown here) of the surfaces of the untreated sample clear show the presence of $\alpha + \beta$ microstructure. After the electron beam treatment, the microstructure of the material becomes in form of α' martensite.



(a)



(b)

Fig. 8. AFM 3D images of TiN/TiO₂ coating deposited on Ti6Al4V a) with EBT and b) without EBT of the substrate

Fig. 8 presents three-dimensional atomic force microscopy (AFM) images of the crystal architecture of the nanostructured uppermost TiO₂ of Ti5Al4V substrates. It is obvious that the electron beam treatment strongly affects the surface roughness. During the EBT process, a liquid/solid interface starts to move along the sample,

which affects the topography of the surface and the roughness of specimen's changes after the solidification. The obtained results for the surface roughness are summarized in Table 1.

It is obvious that the application of electron beam treatment tends to increase the surface roughness about 3 times. From Fig. 8 it is obvious that without the EBT, just a few main surface formations (i.e. peaks or/and valleys) and many secondary ones (with much lower amplitude) exist. After EBT, the surface architecture of main and secondary forms is replaced by relatively uniform peaks and valleys with similar amplitudes. This is attributed to the melting and subsequent rapid solidification of the surfaces. This will lead to a significantly more symmetrical distribution of the measured heights.

The influence of the EBT of Ti5Al4V substrates on the mechanical properties has been studied by nanoindentation tests and the results are summarized in Table 1. The deposited coatings were tested by a load of 50 mN.

Table 1. Statistical parameters of the surface roughness, hardness and modulus of elasticity of the TiN/TiO₂ coatings deposited on electron beam treated and untreated Ti5Al4V substrate

	S _a , nm	S _{sk}	Hardness, GPa	Modulus of elasticity, GPa
Treated substrate	24.757 ± 0.06	-0.20	6.291 ± 1.1	79.040 ± 11.24
Untreated substrate	8.255 ± 0.02	-0.73	7.109 ± 0.57	140.072 ± 8.51

The measured hardness of the TiN/TiO₂ coatings deposited on Ti5Al4V substrate shows that the EBT of the substrate leads to a small decrease of the hardness, namely from 7.109 GPa for the sample without EBT to 6.291 GPa for the specimen with the EBT. This decrease can be explained by the increased surface roughness in the case of EBT of the Ti5Al4V substrate. As the EBT of the Ti5Al4V substrate does not form any changes in the structure of the deposited coatings which correlates with the observed very similar hardness values with and without substrate treatment.

MEASUREMENT OF RESIDUAL STRESSES IN ELECTRON AND LASER BEAM WELDING

Welding is a technological process in which two elements of a structure are joined [24]. It has great application in industry and construction. Welding technology is constantly evolving. Electron beam welding (EBW) [25] and laser beam welding (LBW) are using HEFs.

A very important feature of the welded parts is the level and type of residual stresses and deformations. They have an impact on a number of other features such as service life, load resistance, corrosion resistance, and so on. The measurement of residual stresses is done by various destructive and non-destructive methods. A non-destructive method allowing large depth measurements below the surface of the specimen is the neutron diffraction method [26]. Briefly, the method consists in taking into account the displacement of diffraction maxima in the spectrum of

deformed material versus the non-deformed material spectrum.

The investigated samples were studied on a FSD diffractometer of the impulse reactor IBR-2 at JINR - Dubna, Russia [27].

The objects of our research are various materials welded through HEFs under different technological parameters.

Steel is a very widely used material, both in machine building and in construction.

In the works [28, 29, 30] an analysis of the residual stresses in Sharpy specimens, recovered by electron beam welding (EBW), laser beam welding (LBW) and arc stud welding (ASW) techniques is presented – Fig.9 and Fig.10. The studied material was steel 18MND5. The lowest level of the residual stress was found for EBW specimen as compared to LBW and ASW specimens.

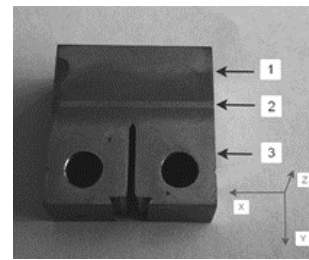


Fig. 9. CT welded specimen (1 – Insert from the test material, 2 – Weld seam, 3 – Holder for CT test) [30]

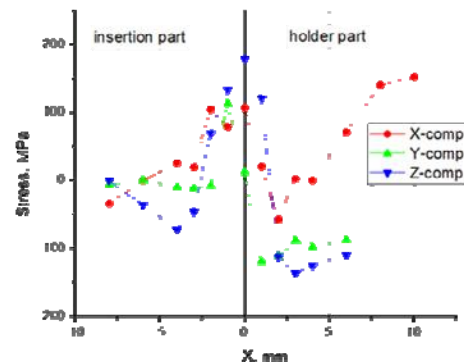


Fig. 10. Residual stress measurement of EBW Sharpy specimen [30]

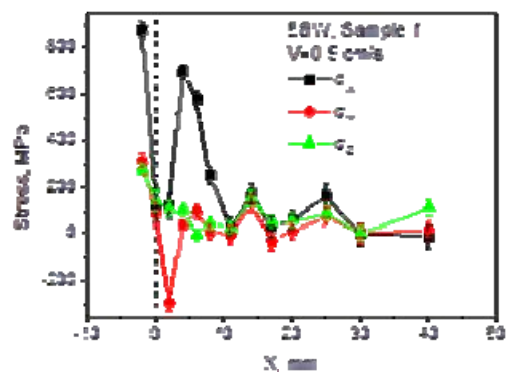


Fig. 11. Residual stress measurement of EBW specimen of constructive steel [31]

The results of the residual stress and microstrain measurements of the EBW constructive steel 12XH3A are

presented in [31]. The results for the one of the three specimens, welded with different welding speed, are shown in Fig.11. It was found that the residual stress level is significantly dependent on welding speed that allows one to optimize welding process by selecting the appropriate parameters. On the contrary, the microstrain level is almost the same for all studied specimens but exhibits slightly different profiles depending on the welding speed.

Gear wheel for transmission of the same steel, welded by electron beam, has been studied by measuring the radial and axial components of the tensor of residual stresses [32] – Fig.12 and Fig. 13. Analysis of diffraction peak broadening gives quite low level of residual microstrain, which ensures the absence of cold cracking in the weld zone. The data will be useful for the analysis of the performance of the built-in gear transmission for cars.

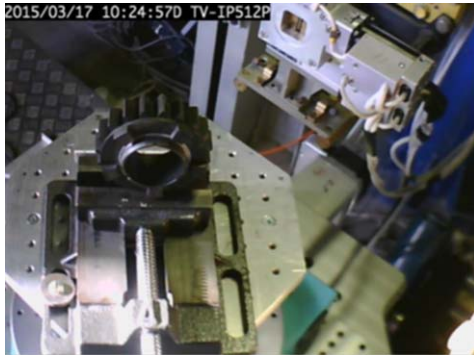


Fig. 12. Photography of the welded gear during the neutron diffraction experiment. [32]

A laser beam welded thin plate of steel C45 was studied and the results have been presented in work [33]. A numerical simulation of residual stresses is also done for this sample.

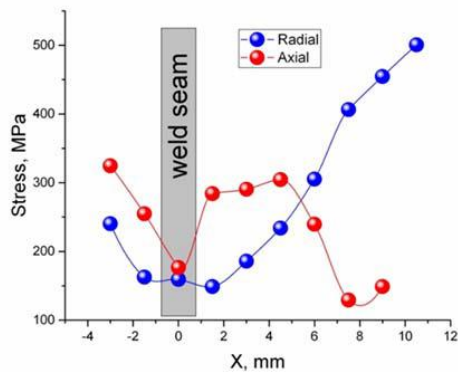


Fig. 13. Residual stress distribution in the sample [32]

Another type of interesting steel is stainless steel. We have examined X5CrNi18-10 chromium-nickel steel with trademark 304. The results for EBW samples with different welding speeds have been reported to UNITECH 2016 [34]. The results for LBW samples from the same steel were presented in work [35]. Three welded specimens of stainless steel 304 with the following chemical composition (wt%): <0.07%C; <1.00%Si; <2.00%Mn; <0.045%P; <0.015%S; 17.0-19.5%Cr; 8.0-10.5%Ni were examined. The samples with size of 100x50x10 mm were welded by 15 kW fiber laser. The technological parameters of the welding process were the following: laser power $Q = 15$ kW; laser spot size $d = 0.65$ mm; welding speed $V = 3$

m/min; 4 m/min 5 m/min, using 30 L/min of protective Ar gas.

Material with very wide application in different fields is aluminum and its alloys. Residual stresses and microdeformation in the EBW of aluminum alloy AMg6 were presented in study [36]. Two specimens were welded with speeds $v=0.5$ cm/s and $v=1.5$ cm/s. X-components of the strain tensor have a low level of residual stresses (~ 75 MPa) in the weld region. The neutron diffraction experiment showed that the width of the heat affected zone is several millimeters.

The welding of dissimilar materials is a difficult task. There are materials that cannot be welded with traditional technology, and EBW successfully solves this problem. Because of the different thermophysical properties of the two joined materials, it is very important to study the residual stresses in both materials. We have researched a welding joint of copper and stainless steel. Two samples welded with different beam current were studied. In Fig. 14 is shown the residual stress distribution in the sample welded with lower beam current.

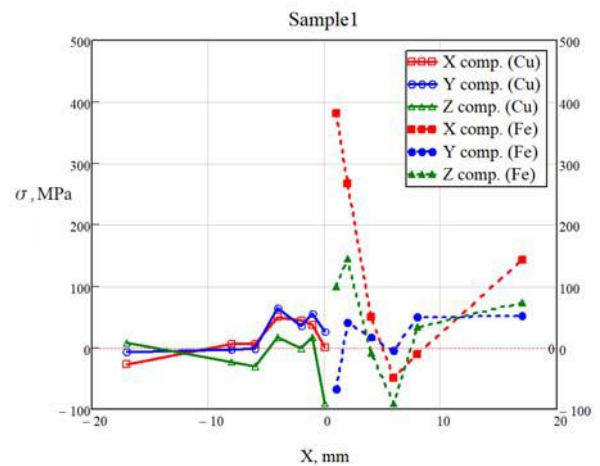


Fig. 14. Residual stress in the studied EBW specimen No. 1. ($I = 50$ mA) [37]

The residual stresses in copper do not exceed 100 MPa in both samples. The maximum stresses can be seen in the steel zone of thermal impact in the X component – 450 MPa. The higher the beam current is, the higher the residual stresses are. The results are presented in work [37].

REFERENCE

- [1] Valkov S, Neov D, Luytov D, Petrov P. Neutron diffraction of titanium aluminides formed by continuous electron-beam treatment. *Journal of Physics: Conference Series*. 2016; 700:012034.
- [2] Valkov S, Bezdushnyi R, Petrov P. Study of the influence of vanadium and niobium on the structure of Ti-Al-V and Ti-Al-Nb alloys formed by selective electron beam alloying. *Journal of Physics: Conference Series*. 2018; 992:012053.
- [3] Valkov S, Bezdushnyi R, Petrov P, Synthesis, structure and mechanical properties of Ti-Al-Nb coatings formed by electron beam additive technique. *Vacuum*. 2018; 156:140-145.
- [4] Lazarova R, Dimitrova R, Murdjieva Y, Valkov S, Petrov P. Layers obtained on aluminum by nanopowder deposition and subsequent electron beam scanning. *Materials and Manufacturing Processes*. 2018;33:1128-1132.
- [5] Almeida A, Carvalho P, Vilar R. Microstructural Study of Al-Cr Alloys Synthesised by Laser Alloying. *Scifed Journal of Metallurgical Science*. 2017;1:1-12

- [6] Petrov P, Vilar R, Almeida A. Laser Surface Alloying of Al with Nb. Surface Modification Technologies In: Proc.8th Int. Conf. Surface Modification Technologies, The Institute of Materials, Nice; 1995, p. 346-353.
- [7] Petrov P, Vilar R, Almeida A. Microstructures and Properties of Al-Nb Alloys Produced by Laser Surface Treatment. In: Laser Processing: Surface Treatment and Film Deposition, Proc. Seminar NATO Advanced Study Institute, Sesimbra, Kluwer Academic Publishers; 1996, p. 565-573.
- [8] Petrov P, Vilar R, Almeida A. A study of the Mechanism Laser Surface Alloying Aluminium with Niobium. Proceedings of SPIE. 1996;3052:357-363.
- [9] Almeida A, Petrov P, Nogueira I, Vilar R. Structure and properties of Al-Nb alloys produced by laser surface alloying. Materials Science and Engineering: A. 2001;303:273-280.
- [10] Valkov S, Petrov P, Lazarova R, Bezdushnyi R, Dechev D. Formation and Characterization of Al-Ti-Nb Alloys by Electron-Beam Surface Alloying. Applied Surface Science. 2016; 389:768-774.
- [11] Valkov S, Petrov P, Lazarova R. Comparative study of electron and laser beam surface alloying. Proceedings of SPIE. 2017;10226: 102260I.
- [12] Vilar R, Conde O, Franco S. Crystallographic structure of Al3Nb in laser-processed Al-Nb alloys. Intermetallics. 1999;7:1227-1233.
- [13] Valkov S, Neov D, Bezdushnyi R, Beskrovnyi A, Kozlenko D, Petrov P. Study of the Microstructure, Crystallographic Structure and Thermal Stability of Al-Ti-Nb Alloys Produced by Selective Electron Beam Alloying. Journal of Surface Investigation: X-ray, Synchrotron and Neutron Techniques. 2018;12:436-441.
- [14] Abbaschian R, Abbaschian L, Reed-Hill R. Physical Metallurgy Principles. 4th ed. Publisher: CL Engineering; 2008.
- [15] Askeland D, Haddleton F, Green P, Robertson H. The Science and Engineering of Materials. 3rd ed. Publisher: Springer US; 1996.
- [16] Grumbt G, Zenker R, Biermann H., Weigel K, Bewilogua K, Bräuer G. Duplex surface treatment – physical vapor deposition (PVD) and subsequent electron beam hardening (EBH). Advanced Engineering Materials. 2014; 16 (5):511-516.
- [17] Hao S, Wang H, Zhao L. Surface modification of 40CrNiMo7 steel with high current pulsed electron beam treatment. Nuclear Instruments and Methods in Physics Research B. 2016; 368:81-85.
- [18] Zenker R, Modern thermal electron beam processes – research results and industrial application. La Metallurgia Italiana. 2009.
- [19] Zenker R, Structure and properties as a result of electron beam surface treatment. Advanced Engineering materials. 2004; 6(7): 581-588.
- [20] Ormanova M, Petrov P, Kovacheva D. Electron beam surface treatment of tool steels. Vacuum. 2017; 135:7-12.
- [21] Ormanova M, Angelov V, Petrov P, Investigation of the thermal processes in electron-beam surface modification by means of a scanning electron beam. Journal of Physics: Conference Series. 2016; 700: 012033.
- [22] Ramskogler C, Warchomicka F, Mostofi S, Weinberg A, Sommitsch C. Innovative surface modification of Ti6Al4V alloy by electron beam technique for biomedical application. Materials Science and Engineering C. 2017; 78: 105-113.
- [23] Petrov P, Dechev D, Ivanov N, Hikov T, Valkov S, Nikolova M, Yankov E, Parshorov E, Bezdushnyi R, Andreeva A. Study of the influence of electron beam treatment of ti5Al4V substrate on the mechanical properties and surface topography of multilayer TiN/TiO2 coatings. Vacuum. 2018 154:264-271
- [24] Mihailov V, Karhin V, Petrov P. Fundamentals of welding (In English). Petersburg: Polytechnic University Publishing, St., 2016.
- [25] Schultz H. Electron beam welding. Cambridge: Abington Publishing, 1994.
- [26] Hutchings M, Withers P, Holden T, Lorentzen T. Introduction to the Characterization of Residual Stress by Neutron Diffraction, Boca Raton:Taylor&Francis Group, 2005
- [27] Bokuchava G. Neutron RTOF Stress Diffractometer FSD at the IBR-2 Pulsed Reactor. Crystals. 2018; 8(8):318. doi:10.3390/cryst8080318.
- [28] Bokuchava G, Papushkin I, Petrov P, Residual stress study by neutron diffraction method in the Sharpy specimens reconstructed by various welding methods. Comptes rendus de l'Académie bulgare des sciences: sciences mathématiques et naturelles. 2014; 67(6):763-768.
- [29] Bokuchava G, Petrov P, Papushkin I, Application of Neutron Stress Diffractometry for Studies of Residual Stresses and Microstrains in Reactor Pressure Vessel Surveillance Specimens Reconstituted by Beam Welding Methods. Journal of Surface Investigation: X-ray, Synchrotron and Neutron Techniques.2016; 10(6):1143–1153.
- [30] Papushkin I, Kaisheva D, Bokuchava G, Angelov V, Petrov P. Study of residual stresses in CT test specimens welded by electron beam. Journal of Physics: Conference Series.2018; 992:012016.
- [31] Petrov P, Kaisheva D, Bokuchava G, Papushkin I. A neutron diffraction study of residual stress due to electron beam welding, In: Proceedings of the 3-rd IIW South-East European Welding Congress, 2015, p.108-112.
- [32] Papushkin I, Kaisheva D, Bokuchava G, Petrov P. Evaluation of Residual Stress and Microstrain in Electron Beam Welded Gear Wheel by Neutron Diffraction, In: Proceedings of the XXVIII International Scientific Conference of Faculty Industrial Technology, 2015, p. 131-136.
- [33] Petrov P, Bokuchava G, Papushkin I, Genchev G, Doynov N, Michailov V, Ormanova M. Neutron diffraction studies of laser welding residual stresses, In: Proceedings of SPIE, 2017,10226D.
- [34] Petrov P, KaishevaD, Bokuchava G, Papushkin I. Study of residual stresses in electron beam welding of chrome-nickel steel by diffraction of neutron pulse flow, In: Proceedings - UNITECH 2016, Vol. 3, 2016, p. 174-176.
- [35] Kaisheva D, Bokuchava G, Papushkin I, Genchev G, Doynov N, Ossenbrink R, Michailov V, Petrov P, Determination of residual stresses in fiber laser welded stainless steel joints by neutron diffraction method, In: Proceedings of SPIE, 2018, (accepted, in press).
- [36] Kaisheva D, Papushkin I, Bokuchava G, Petrov P, Study of Residual Stresses in Electron Beam Welded Samples of an Aluminum Alloy via Neutron Diffraction Method, In: AIP Conference Proceedings, 2018, (accepted, in press).
- [37] Petrov P, Kaisheva D, Bokuchava G, Papushkin I, Valkov S, Investigation of Residual Stresses in Dissimilar Copper-Steel Joint Welded by Electron Beam, In: Proceedings of the 4-th IIW South-East European Welding Congress, 2018, (accepted, in press).